Sensitive detection of CO_2 concentration and temperature for hot gases using quantum-cascade laser absorption spectroscopy near 4.2 μm

Kuijun Wu · Faquan Li · Xuewu Cheng · Yong Yang · Xin Lin · Yuan Xia

Abstract Mid-infrared quantum-cascade laser (QCL) absorption spectroscopy of CO_2 near 4.2 μm has been developed for measurement of temperature and concentration in hot gases. With stronger absorption line-strengths than transitions near 1.5, 2.0, and 2.7 μm used previously, the fundamental band $(00^01–00^00)$ of CO_2 near 4.2 μm provides greatly enhanced sensitivity and accuracy to sense CO_2 in high-temperature gases. Line R(74) and line R(96) are chosen as optimum pair for sensitive temperature measurements due to their high-temperature sensitivity, equal signal-to-noise ratio (SNR), weak interference of H_2O transitions, as well as relatively strong line-strengths in high temperature and weak absorption in room temperature. The high-resolution absorption spectrum of the far wings of the R-branch (R56–R100) in the fundamental vibrational band of CO_2 is measured in a heated cell over the range 2,384–2,396 cm^{-1} at different temperatures from 700 to 1,200 K. Taking three factors into consideration, including SNR, concentration detectability, and uncertainty sensitivity, the absorption line R(74) is selected to calculate CO_2 concentration. The tunable QCL absorption sensor is validated in mixtures of CO_2 and N_2 in a static cell for temperature range of 700–1,200 K, achieving an accuracy of ±6 K for temperature and ±5 % for concentration measurements.

K. Wu · F. Li (✉) · X. Cheng · Y. Yang · X. Lin · Y. Xia
State Key Laboratory of Magnetic Resonance and Atomic and Molecular Physics, Wuhan Institute of Physics and Mathematics, Chinese Academy of Sciences, Wuhan National Laboratory for Optoelectronics, Wuhan 430071, China
e-mail: lifaquan@wipm.ac.cn

K. Wu · X. Lin · Y. Xia
University of Chinese Academy of Sciences, Beijing 100049, China

1 Introduction

Laser-based combustion diagnostics methods, such as laser-induced fluorescence [1], Rayleigh and Raman scattering techniques [2], coherent anti-Stokes Raman scattering [3], cavity ring-down absorption spectroscopy [4], supercontinuum absorption spectroscopy [5], Fourier-domain mode-locked laser absorption spectroscopy [6], as well as tunable diode laser absorption spectroscopy (TDLAS) [7–12], have stimulated drastic research interest during the past two decades for their nonintrusive nature and in situ measurement capability. TDLAS is highly sensitive for monitoring gas concentration and temperature in combustion environment and has been widely used in modern combustion and propulsion to reduce pollutant emissions or improve combustion efficiency. Sun et al. [11] reported the first TDLAS absorption sensor for measurements of gas temperature and species concentration in a slagging coal gasifier. Huang et al. [12] reported an in situ optical system for real-time CO concentration measurement of industrial flame using near-infrared tunable diode laser with direct and modulated absorption signals.

CO_2 is a primary product emission from combustion devices and an important indicator of combustion efficiency. Previous CO_2 sensors are based on TDLAS technology, using transitions of combination bands in near-infrared region, such as 1.5 $(22^01–00^00)$ [8], 2.0 $(12^01–00^00)$ [9, 11, 13, 14], or 2.7 μm $(10^01–00^00)$ [15–17]. However, these absorption bands are relatively weak at combustion-like temperatures (T > 600 K), and therefore have limited range and applicability, especially in gas systems at elevated combustion-like temperature, wherein CO_2 is not a major component, which restricts the applicability of TDLAS technology in some combustion diagnostics systems.

The recent commercial availability of high-power, room-temperature, narrow line-width, single-mode and mode-hop-free (MHF) tunable IR laser sources, and quantum-cascade lasers (QCL) offers the possibility of applying high-sensitivity and high-resolution mid-IR absorption spectroscopy on combustion diagnostics. QCL-based concentration and temperature sensors for combustion gases, such as CO [18–20], H_2O [21], and NO [22, 23], have been reported previously. Vanderover and Oehlschlaeger [18] described the first QCL-based mid-IR laser absorption sensor for CO mole fraction and temperature measurements from 900 to 4,000 K, using line pairs near the intensity peak of CO fundamental band at 4.6 μm. Chao et al. [22, 23] demonstrated a mid-IR absorption strategy for real-time, in situ detection of NO in combustion exhaust gases and measured the H_2O absorption spectroscopy at 633 K in the effluent of a fuel-lean C_2H_4/air flame [23] using an external-cavity QCL working at the fundamental absorption band of NO near 5.2 μm. More recently, Spearrin et al. [24] reported their progress in multi-band infrared CO_2 absorption sensor using the R(28) line of combination band (10^01–00^00) near 2.7 μm and the R(96) line of fundamental band (00^01–00^00) near 4.2 μm, and their cross-band two-line thermometry technique provided greatly enhanced sensitivity and widely expanded useful range for high-temperature measurement. However, the R(28) line (near 3,633.08 cm^{-1}), with a relatively low value of lower-state energy (about 316.77 cm^{-1}) and a relatively high value of reference line-strength (about 0.59 cm^{-2} atm^{-1}) [25], has a non-ignorable absorption coefficient (about 0.0012 cm^{-1}) at room temperature, 10 times stronger than that at 1,500 K, which may reduce the sensor accuracy or lead to greater measurement uncertainty.

The absorption line-strengths of CO_2 and H_2O in the near-infrared (near-IR) and mid-infrared (mid-IR) region at 1,500 K are shown in Fig. 1 [25]. Compared with combination bands near 1.5, 2.0, and 2.7 μm used in previous CO_2 sensors, the fundamental band (00^01–00^00) near 4.2 μm is promising for sensitive detection, especially in conditions of relatively low CO_2 concentration or short path length, due to its relatively strong line-strengths and weak interference of H_2O transitions.

In this paper, we describe a QCL-based mid-IR absorption sensor for CO_2 concentration and temperature, operating near 4.2 μm. This sensor is designed to achieve a greatly enhanced sensitivity and accuracy in measuring CO_2 in high-temperature gases with little interference of H_2O transitions and weak influence from cold boundary layer. Strong line-strengths, high-temperature sensitivity, and equal signal-to-noise ratio (SNR) are taken into account in optimum pair selection for sensitive temperature measurements. By measuring the high-resolution
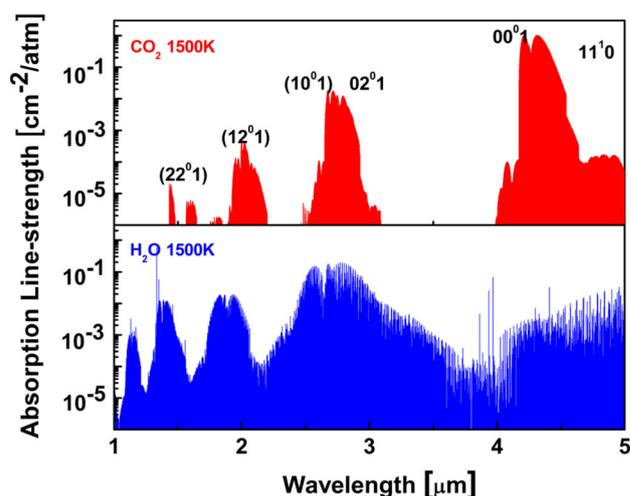

Fig. 1 Absorption line-strengths of CO_2 and H_2O at 1,500 K [25]

absorption spectrum of the fundamental transitions and using two-line thermometry technique, sensing of gas temperature is carried out. In order to improve the detection sensitivity and accuracy of CO_2 concentration, concentration detectability, uncertainty sensitivity, and SNR are taken as major factors in optimum absorption line selection for accurate CO_2 concentration calculation. These quantitative validation measurements confirm the potential application of QCL-based mid-IR absorption strategy for CO_2 concentration and temperature measurement in combustion environments.

2 Theory

2.1 Fundamental spectroscopy

The fundamental theoretical principle of absorption spectroscopy, which describes the relationship between transmitted and incident spectral intensities, is given by the Beer-Lambert law equation [15]:

$$T_v = \left(\frac{I}{I_0}\right)_v = \exp\left[-NL\sum_i S_i(T)\Phi(v - v_i)\right]. \tag{1}$$

where, T_v is the transmission; I and I_0 are the transmitted and incident laser intensities, respectively; N is the number density of the absorbing species; L is the total absorption path length; $S_i(T)$ and $\Phi(v - v_i)$ denote the line-strength and line-shape of a particular transition i, respectively. Here, v_i is the center frequency of various absorption lines, and v is the scanned laser frequency.

The absorption line-shape $\Phi(v - v_i)$, influenced by both homogeneous collision broadening and inhomogeneous

Doppler broadening, can be given by Voigt profile, which is constituted by both Lorentzian and Gaussian functions. No matter how strongly the collision and Doppler broadening terms influence the absorption line-shape, the Voigt function is area-normalized in such a way that $\int_v \Phi(v - v_i)dv \equiv 1$.

The absorption line-shape, $S_i(T)$, has a temperature dependence:

$$S_i(T) = S_i(T_0)\frac{Q(T_0)}{Q(T)}\exp$$
$$\left[\frac{-hcE_i''}{k_B}\left(\frac{1}{T} - \frac{1}{T_0}\right)\frac{1 - \exp\left(\frac{-hcv_i}{k_BT}\right)}{1 - \exp\left(\frac{-hcv_i}{k_BT_0}\right)}\right]. \tag{2}$$

In the above expression, $S_i(T_0)$ is reference line-strength at reference temperature $T_0 = 296$ K, $Q(T)$ is the partition function, E_i'' is the lower-state energy of transition i, and h, c, k_B are Plank's constant, speed of light, and Boltzmann constant, respectively.

This mid-IR laser absorption sensor for temperature measurement is based on scanned-wavelength direct absorption (DA) and two-line ratio technique with a single room-temperature QCL. Temperature can be inferred from the integrated absorbance ratio of two different transitions of the same species [26]. The ratio R of two integrated absorbance (A_1 and A_2) is given by the following equation:

$$R = \frac{A_1}{A_2} = \frac{S_1(T)}{S_2(T)}$$
$$= \frac{S_1(T_0)}{S_2(T_0)}\exp\left[-\left(\frac{hc}{k_B}\right)(E_1'' - E_2'')\left(\frac{1}{T} - \frac{1}{T_0}\right)\right]. \tag{3}$$

Therefore, temperature T can be obtained and described as

$$T = \frac{\frac{hc}{k_B}(E_2'' - E_1'')}{\ln\frac{A_1}{A_2} + \ln\frac{S_2(T_0)}{S_1(T_0)} + \frac{hc}{k_B}\frac{(E_2'' - E_1'')}{T_0}}. \tag{4}$$

With the calculated temperature known, the CO$_2$ concentration could then be inferred from either line of these two candidate transitions using the equation

$$X = \frac{A}{PS(T)L}, \tag{5}$$

where, A is the integrated absorbance, and P is the pressure.

2.2 Line selection

It is important to select the optimal spectral line pair for the mid-IR absorption sensor, which is based on the two-line ratio technique. Systematic line-selection criteria rules for tunable diode laser (TDL) temperature sensor have been introduced by Liu et al. [26]. Those selection rules will be adopted and developed for our design of mid-IR absorption sensor in this section. Not limited to the spectral region of 1.3–1.5 μm, where fiber-coupled telecommunication lasers are commercially available, CO$_2$ fundamental band (00^01–00^00) is selected as candidate transitions, which has been briefly discussed in the Introduction section. In the spectral region of 4–5 μm, absorption lines near 4.2 μm are relatively free of interference from high-temperature H$_2$O transitions, as shown in Fig. 1.

The influence of water interference and atmospheric absorption is further illustrated in Fig. 2. As can be seen from Fig. 2b and c, the interference of H$_2$O transitions is negligible, considering that the absorbance of H$_2$O is 200 times lower than that of CO$_2$, over the wavenumber range of 2,384–2,396 cm^{-1}. And those 22 transitions in the far wings of the R-branch (R58–R100) keep free of interference absorption from H$_2$O, unless the concentration ratio of H$_2$O to CO$_2$ reaches 50:1. However, it should be noticed that the interference of room air CO$_2$ could not be neglected for its relatively strong absorption in the 2,384–2,388 cm^{-1} range, which can be seen from Fig. 2a. Therefore, 14 transitions of CO$_2$ R(74)–R(100) that appear in the 2,388–2,396 cm^{-1} range are identified as the main group of candidate lines for optimum detection of CO$_2$ in hot, humid media.

In order to avoid the interference caused by the overlap of adjacent absorption features at atmospheric pressure, the spectral separation range of the two nearby transitions must be >0.3 cm^{-1} [27]. Some basic information about these 14 candidate transitions mentioned above is compiled in Table 1 [25]. Two promising absorption lines R(98) and R(100) are rejected, due to their potential interference from neighboring transitions.

In addition, the temperature dependence of absorption lines must also be taken into consideration before designing the combustion sensor. Generally, the line-strength fluctuation of transitions with lower rotational states is larger than those with higher rotational states. Therefore, many absorption lines have a similar magnitude line-strength for temperatures typical of combustion gases, as illustrated in Fig. 3.

The temperature sensitivity of two-line ratio technique, defined as the unit change in line-strength ratio for a unit change in temperature, can be obtained by the following differentiating equation [27]:

$$\left|\frac{\partial R/R}{\partial T/T}\right| = \frac{hc}{k}\frac{\left|(E_2'' - E_1'')\right|}{T} \tag{6}$$

It can be seen from this equation that a large difference in lower-state energy of a line pair is desired to have high-

Fig. 2 Simulated transmission spectra of CO_2 at room-temperature and absorption spectra of H_2O and CO_2 at high-temperature at conditions of:
a $P = 1$ atm, $T = 300$ K, $L = 5$ m, $X_{CO2} = 400$ ppm;
b $P = 1$ atm, $T = 1,500$ K, $L = 0.1$ m, $X_{H2O} = 5$ %;
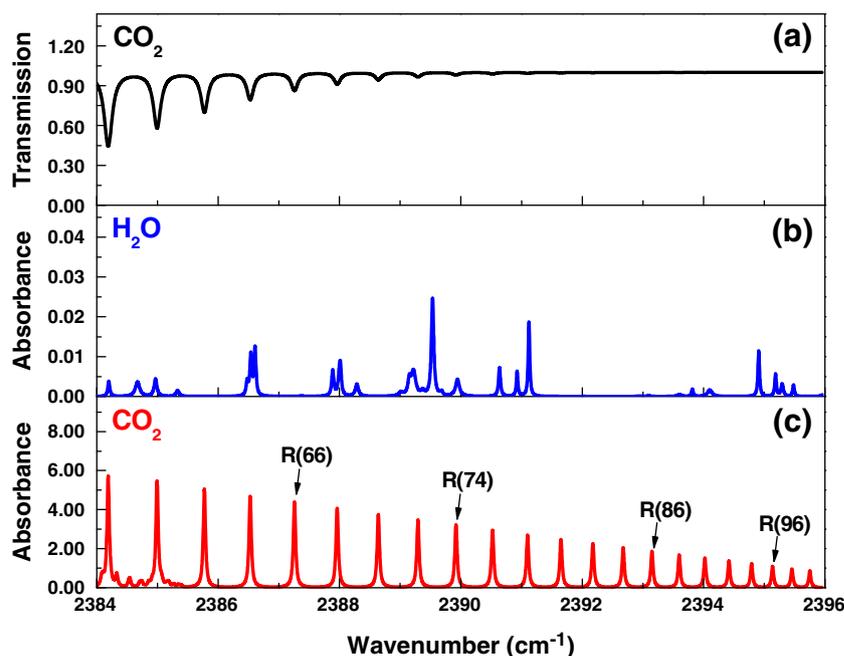**c** $P = 1$ atm, $T = 1,500$ K, $L = 0.1$ m, $X_{CO2} = 5$ %

Table 1 The parameters of candidate CO_2 transitions [25]

Frequency (cm^{-1})	Line intensity (cm^{-2} atm^{-1})	Lower-state energy (cm^{-1})	Transition
2,389.92	0.4483	2,161.61	R(74)
2,390.52	0.4111	2,279.00	R(76)
2,391.10	0.3757	2,399.47	R(78)
2,391.65	0.3420	2,523.02	R(80)
2,392.18	0.3104	2,649.66	R(82)
2,392.68	0.2806	2,779.37	R(84)
2,393.15	0.2528	2,912.16	R(86)
2,393.60	0.2270	3,048.02	R(88)
2,394.02	0.2030	3,186.95	R(90)
2,394.42	0.1810	3,328.96	R(92)
2,394.79	0.1608	3,474.03	R(94)
2,395.14	0.1423	3,622.16	R(96)
2,395.46	0.1255	3,773.36	R(98)
2,395.75	0.1106	3,927.62	R(100)

Fig. 3 Line-strength for the 12 transitions of CO_2 R(74)–R(96) as a function of temperature

temperature sensitivity. As displayed by Table 1, lower-state energy of the transitions increases with rotational quantum number, which means that the difference of lower-state energy also increases with the difference of rotational quantum number. However, the detection of optimal line pair is also limited by the line-strength ratio of the two absorption lines [28], because equal SNR is desired for both measurements. To characterize the performance of this two-line temperature sensor, the line-strength ratio and temperature sensitivity of the two transitions R(74) and R(96) are plotted in Fig. 4 as a function of temperature. Typically, the line-strength ratio should not be too far from
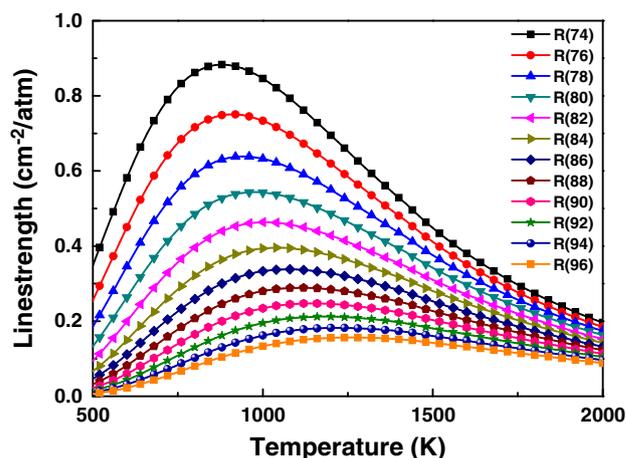
unity, and the sensitivity should at least be one for sensitive temperature measurements. These two curves indicate that this line pair can be used for accurate temperature sensing at elevated temperatures between 700 and 2,000 K.

3 Experiments

3.1 Spectroscopic measurements

The commercial continuous wave external-cavity QCL from Daylight Solutions used for this work can be tuned over the range of 2,275–2,420 cm^{-1} (4.1322–4.3956 μm) at a thermoelectrically cooled chip temperature of 18 °C
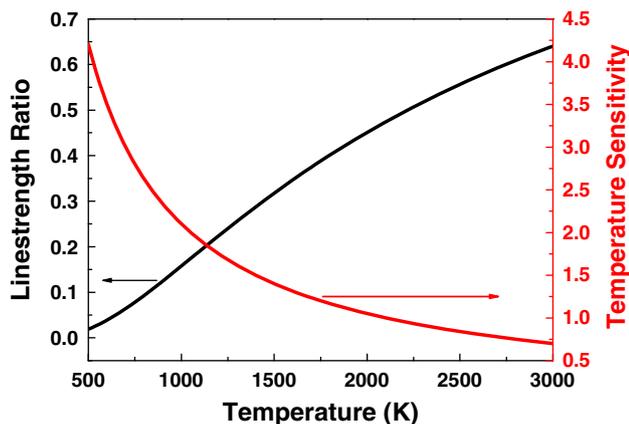
Fig. 4 Line-strength ratio and temperature sensitivity for the line pair R(74) and R(96) of CO_2

Fig. 5 The schematic illustration of the experimental arrangement used for measuring CO_2 DA spectroscopy in a heated static cell

and working current of 600 mA, and within this tuning range, a MHF region of over 70 cm^{-1} is available. The laser can be scanned over the entire wavenumber range using the laser controller with 6 different preset tuning rates for the grating inside the laser head. This laser is single-mode, with a line-width <0.001 cm^{-1} and output power more than 150 mW, which makes it an ideal monochromatic light source for high-sensitivity and high-resolution spectroscopy on IR-active fundamental rovibrational transitions of molecules like CO_2.

The schematic of the experimental arrangement used for measuring CO_2 DA spectroscopy in a heated static cell is shown in Fig. 5. The laser beam was split into a sample channel and a reference one. The sample beam transmitted through the three-section cell with sample gas and was detected by a thermoelectrically cooled mercury cadmium telluride (MCT) detector (VIGO PVI-3-TE-6). The reference beam transmitted through the free space and was detected by a same detector. Both detectors' built-in pre-amplifiers (VIGO MIPDC-F-20) had a bandwidth of 20 MHz. The output of each detector preamplifier was sent to a 1 G sample/s, 100 MHz bandwidth digital oscilloscope (Tektronix DPO 2014) with a sampling rate of 12.5 kHz. A band-pass optical filter (Spectrogon BP-4240-200 nm) was placed in front of the detector to reduce the emission noise from the high-temperature furnace and heated cell. The three-section cell was placed inside the heated furnace. The center section cell with a path length of 20.0 cm was filled with test gas and located in the uniform-temperature region of the furnace, while these two outer section cells were full of N_2 to minimize temperature gradients and avoid interference by ambient CO_2. The temperature and the pressure of the cell were measured by a type-K thermocouple and a pressure gauge. The wavelength and intensity of this QCL were controlled by a temperature and current controller from Daylight Solutions.
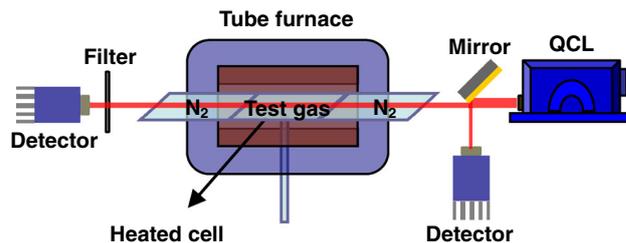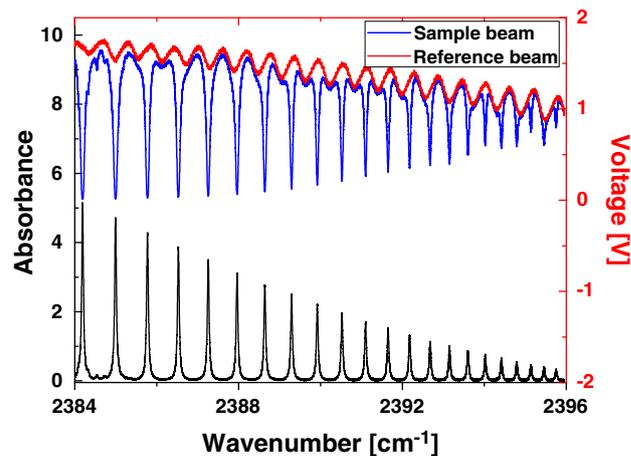

Fig. 6 Upper trace, the reflected laser intensity of the reference beam, as well as the transmitted laser intensity of the sample beam; Lower trace, the analyzed absorption spectrum, between the range 2,384–2,396 cm^{-1} at the experimental conditions of $T = 1,100$ K, $P = 0.95$ atm, $L = 20.0$ cm and $X_{CO2} = 1.19$ %

The wavelength scanning range of the external-cavity laser accessed the far wings of the R-branch (R58–R100) in the fundamental vibrational band of CO_2 near 4.2 μm and scanned at a rate of 10 cm^{-1}/s. The absorption features of CO_2 between the range 2,384–2,396 cm^{-1} are measured at different temperatures from 700 to 1,200 K. Figure 6 shows the reflected laser intensity of the reference beam, as well as the transmitted laser intensity of the sample beam, through a 20.0-cm-long cell filled with 0.95 atm of 1.19 % CO_2 at 1,100 K in the upper trace and the processed absorption spectrum in the lower trace.

3.2 Temperature and concentration measurement

Figure 7 compares the measured absorption spectrum and best-fit Voigt profile of the candidate line pair R(74) and R(96), at the experimental conditions of $T = 1,200$ K, $P = 0.8$ atm, $L = 20.0$ cm and CO_2 concentration of 1.2 %. Also shown in Fig. 7 are the residuals of the

Fig. 7 Experimental data and best-fit Voigt profile for line R(74) and R(96) at the experimental conditions of $T = 1,200$ K, $P = 0.8$ atm, $L = 20.0$ cm, and CO_2 concentration of 1.2 %
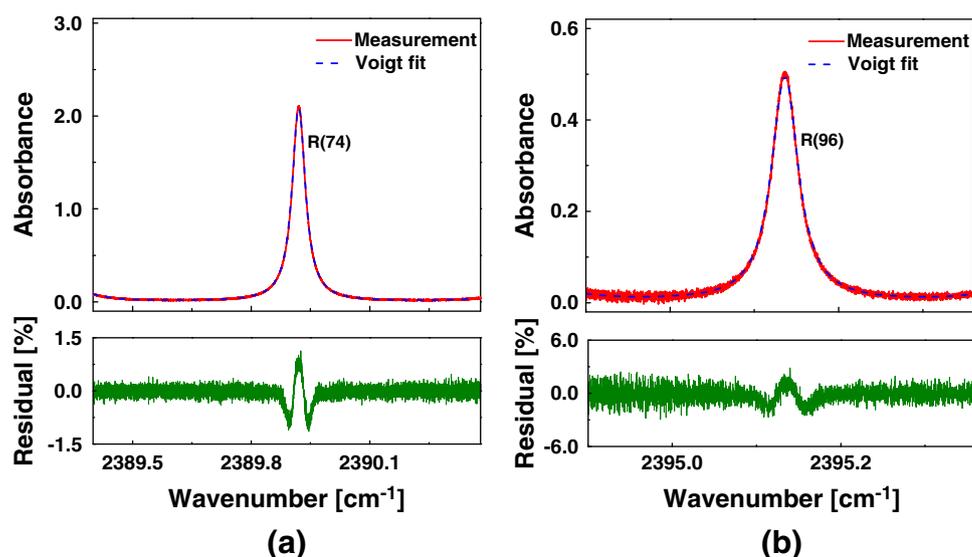
experimental data and Voigt fit. Good agreement between the measured absorption spectrum and best-fit Voigt profile indicates that the Voigt profile adequately models the absorption line-shape under the experimental condition.

Wavelet-based de-noising technique was applied to our QCL absorption sensor in post-signal processing to remove stochastic noise from the QCL and detectors and improve the SNR of the raw spectra. The SNR of line R(74) is about 40 dB, while that for line R(96) is about 28 dB. The peak-normalized residual values for these two candidate transitions are about 1.1 % and 3.1 %, respectively.

With the absorption spectroscopy measured and the ratio of integrated areas calculated, the temperature in the heated static cell could be obtained by using the Eq. 4, and the CO_2 concentration could then be inferred from either line of these two candidate transitions using Eq. 5, with test temperature being known. However, it is necessary to select a more suitable absorption line from candidate transitions R(74) and R(96), considering the detection sensitivity and accuracy of CO_2 concentration.

Figure 8 shows the concentration detectability and uncertainty sensitivity of absorption lines R(74) and R(96). The variations of the integrated absorbance with CO_2 concentration at 1,200 K and 0.5 atm for line R(74) and R(96) are illustrated in Fig 8a. According to the theoretical analysis of Zhou et al. [28] and the experimental result reported by Chao et al. [23], sufficient signal for quantitative detection will be obtained, if the SNR is >10, which requires that the absorbance detection limit exceeds 10^{-3}. Therefore, the absorption line R(74) is more likely to provide a relatively better concentration detectability. Figure 8b plots the simulated concentration uncertainty caused by the temperature measurement error with a typical value of 1 %, which indicates that line R(96) is

relatively insensitive to the temperature measurement error from 1,100 to 2,000 K. Taking those three factors into consideration, including SNR, concentration detectability, and uncertainty sensitivity, absorption line R(74) is selected to compromise these opposing demands.

Experiments are performed under different experimental conditions to measure gas temperature and CO_2 concentration, and the results with comparison to the known values are plotted in Fig. 9. The upper panel compares the thermocouple measurements with the temperatures measured by the QCL absorption spectroscopy sensor, and the lower panel shows the ratio of the CO_2 concentration measured by the QCL absorption spectroscopy sensor and the known mixture concentration. Both the temperature and the CO_2 concentration measured by the QCL absorption spectroscopy sensor agree well with the known values over the entire temperature range 700–1,200 K with a deviation of ±6 K and ±5 %, respectively. These quantitative validation measurements confirm the potential application of QCL-based mid-IR absorption strategy for CO_2 concentration and temperature measurement in combustion environments.

4 Summary

QCL-based mid-IR absorption sensor for CO_2 concentration and temperature at combustion-like temperature were reported using the fundamental band of CO_2 near 4.2 μm. High-temperature absorption spectra of CO_2 and H_2O and room-temperature atmospheric transmittance were simulated to obtain suitable CO_2 transitions for combustion monitoring. Two absorption lines, R (74) and R (96), belonging to the $(00^01–00^00)$ rovibrational band were

Fig. 8 The concentration detectability and uncertainty sensitivity of line R(74) and R(96): **a** variations of the integrated absorbance with CO_2 concentration at 1,200 K and 0.5 atm for line R(74) and R(96); **b** the simulated concentration uncertainty caused by the temperature measurement error with a typical value of 1 %
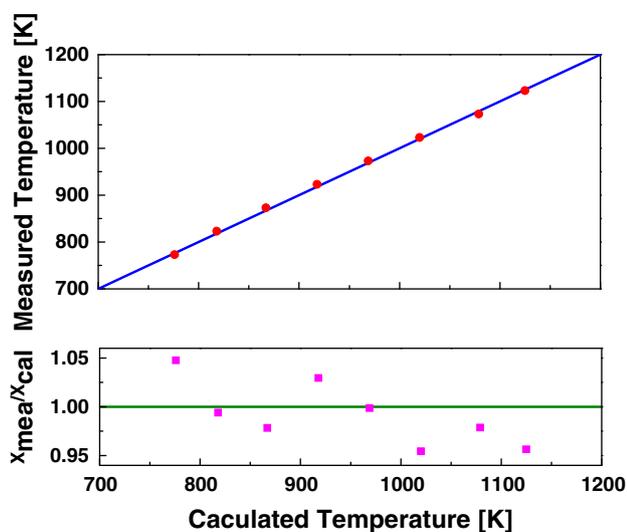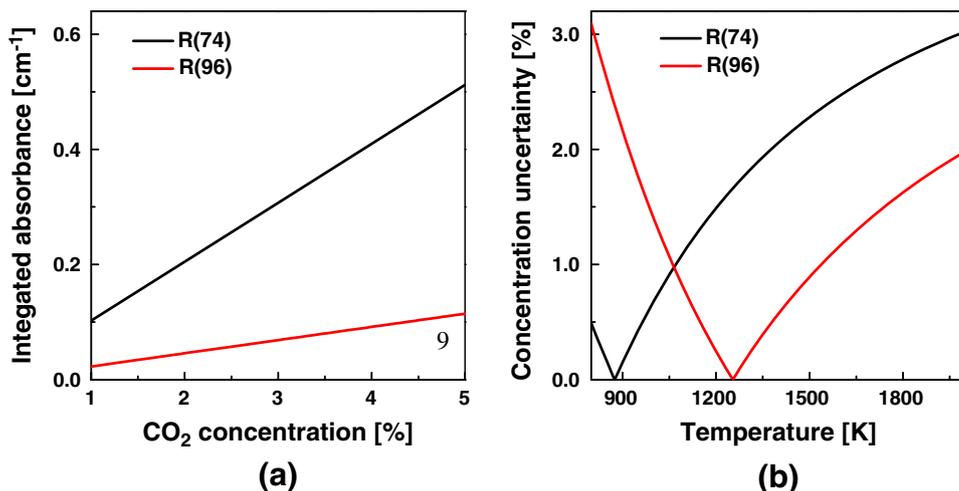

(a)

(b)

Fig. 9 Validation measurements of gas temperature and CO_2 concentration in the well-controlled static cell

selected as optimum line pair for their equal SNR, high-temperature sensitivity, and freedom from interference of neighboring CO_2 and H_2O transitions. The absorption features of CO_2 between the range 2,384–2,396 cm^{-1} were measured, and good agreement between the measured spectrum and the Voigt profile was obtained. The absorption line R(74) was selected to calculate CO_2 concentration to improve detection sensitivity and accuracy for its relatively higher SNR and better concentration detectability. This scanned-wavelength DA CO_2 temperature sensor was validated in a mixture of CO_2 and N_2 in a static cell for temperature range of 700–1,200 K, achieving an accuracy of ±6 K for temperature and ±5 % for CO_2 concentration measurements. In the future, we are planning to extend this scanned-wavelength DA sensor to fixed-wavelength one

for capture the rapid change of gas properties in chemical reactions, and apply the developed sensor to measurements in practical combustion devices.

References

1. K. Kohse-Höinghaus, Laser techniques for the quantitative detection of reactive intermediates in combustion systems. Prog. Energy Combust. Sci. **20**, 203 (1994)
2. N.M. Laurendeau, Temperature measurements by light-scattering methods. Prog. Energy Combust. Sci. **14**, 147 (1988)
3. F. Beyrau, T. Seeger, A. Malarski, A. Leipertz, Determination of temperatures and fuel/air ratios in an ethene–air flame by dual-pump CARS. J. Raman Spectrosc. **34**, 946 (2003)
4. J. Luque, P.A. Berg, J.B. Jeffries, G.P. Smith, D.R. Crosley, J.J. Scherer, Cavity ring-down absorption and laser-induced fluorescence for quantitative measurements of CH radicals in low-pressure flames. Appl. Phys. B **78**, 93 (2004)
5. T. Werblinski, S.R. Engel, R. Engelbrecht, L. Zigan, S. Will, Temperature and multi-species measurements by supercontinuum absorption spectroscopy for IC engine applications. Opt. Express **21**, 13656 (2013)
6. L.A. Kranendonk, X. An, A.W. Caswell, R.E. Herold, S.T. Sanders, R. Huber, J.G. Fujimoto, Y. Okura, Y. Urata, High speed engine gas thermometry by Fourier-domain mode-locked laser absorption spectroscopy. Opt. Express **15**, 15115 (2007)
7. D.S. Baer, R.K. Hanson, M.E. Newfield, N.K.L.M. Gopaul, Multiplexed diode-laser sensor system for simultaneous H_2O, O_2, and temperature measurements. Opt. Lett. **19**, 1900 (1994)
8. R.M. Mihalcea, D.S. Baer, R.K. Hanson, Diode laser sensor for measurements of CO, CO_2, and CH_4 in combustion flows. Appl. Opt. **36**, 8745 (1997)
9. M.E. Webber, J. Wang, S.T. Sanders, D.S. Baer, R.K. Hanson, In situ combustion measurements of CO, CO_2, H_2O and temperature using diode laser absorption sensors. Proc. Combust. Inst. **28**, 407 (2000)
10. H. Teichert, T. Fernholz, V. Ebert, Simultaneous in situ measurement of CO, H_2O, and gas temperatures in a full-sized coal-fired power plant by near-infrared diode lasers. Appl. Opt. **42**, 2043 (2003)
11. K. Sun, R. Sur, X. Chao, J.B. Jeffries, R.K. Hanson, R.J. Pummill, K.J. Whitty, TDL absorption sensors for gas temperature

and concentrations in a high-pressure entrained-flow coal gasifier. Proc. Combust. Inst. **34**, 3593 (2013)

12. Q. Huang, F. Wang, H. Zhang, J. Yan, M. Ni, K. Cen, In-situ CO measurement of gas and oil combustion flame using near infrared tunable diode laser with direct and modulated absorption signals. Opt. Commun. **306**, 99 (2013)

13. R.M. Mihalcea, D.S. Baer, R.K. Hanson, Diode-laser absorption measurements of CO_2 near 2.0 μm at elevated temperatures. Appl. Opt. **37**, 8341 (1998)

14. M.E. Webber, S. Kim, S.T. Sanders, D.S. Baer, In situ combustion measurements of CO_2 by use of a distributed-feedback diode-laser sensor near 2.0 μm. Appl. Opt. **40**, 821 (2001)

15. A. Farooq, J.B. Jeffries, R.K. Hanson, Concentration and temperature sensor for combustion gases using diode-laser absorption near 2.7 μm. Appl. Phys. B **90**, 619 (2008)

16. A. Farooq, J.B. Jeffries, R.K. Hanson, Sensitive detection of temperature behind reflected shock waves using wavelength modulation spectroscopy of CO_2 near 2.7 μm. Appl. Phys. B **96**, 161 (2009)

17. R.M. Spearrin, C.S. Goldenstein, J.B. Jeffries, R.K. Hanson, Fiber-coupled 2.7 μm laser absorption sensor for CO_2 in harsh combustion environments. Meas. Sci. Technol. **24**, 055107 (2013)

18. J. Vanderover, M.A. Oehlschlaeger, A mid-infrared scanned-wavelength laser absorption sensor for carbon monoxide and temperature measurements from 900 to 4000 K. Appl. Phys. B **99**, 353 (2010)

19. W. Ren, A. Farooq, D.F. Davidson, R.K. Hanson, CO concentration and temperature sensor for combustion gases using quantum-cascade laser absorption near 4.7 μm. Appl. Phys. B **107**, 849 (2012)

20. R.M. Spearrin, C.S. Goldenstein, J.B. Jeffries, R.K. Hanson, Quantum cascade laser absorption sensor for carbon monoxide in high-pressure gases using wavelength modulation spectroscopy. Appl. Opt. **53**, 1938 (2014)

21. A.K. Das, M. Uddi, C. Sung, Two-line thermometry and H_2O measurement for reactive mixtures in rapid compression machine near 7.6 μm. Combust. Flame **159**, 3493 (2012)

22. X. Chao, J.B. Jeffries, R.K. Hanson, Wavelength-modulation-spectroscopy for real-time, in situ NO detection in combustion gases with a 5.2 μm quantum laser. Appl. Phys. B **106**, 987 (2012)

23. X. Chao, J.B. Jeffries, R.K. Hanson, In situ absorption sensor for NO in combustion gases with a 5.2 μm quantum-cascade laser. Proc. Combust. Inst. **33**, 725 (2011)

24. R.M. Spearrin, W. Ren, J.B. Jeffries, R.K. Hanson, Multi-band infrared CO_2 absorption sensor for sensitive temperature and species measurements in high-temperature gases. Appl. Phys. B (2014). doi:10.1007/s00340-014-5772-7

25. L. Rothman, I.E. Gordon, Y. Babikov, A. Barbe, D. Benner, P.F. Bernath, M. Birk, L. Bizzocchi, V. Boudon, L.R. Brown, A. Campargue, K. Chance, E.A. Cohen, L.H. Coudert, V.M. Devi, B.J. Drouin, A. Fayt, J.-M. Flaud, R.R. Gamache, J.J. Harrison, J.-M. Hartmann, C. Hill, J.T. Hodges, D. Jacquemart, A. Jolly, J. Lamouroux, R.J. LeRoy, G. Li, D.A. Long, O.M. Lyulin, C.J. Mackie, S.T. Massie, S. Mikhailenko, H.S.P. Müller, O.V. Naumenko, A.V. Nikitin, J. Orphal, V. Perevalov, A. Perrin, E.R. Polovtseva, C. Richard, M.A.H. Smith, E. Starikova, K. Sung, S. Tashkun, J. Tennyson, G.C. Toon, V.G. Tyuterev, G. Wagner, The HITRAN2012 molecular spectroscopic database. J. Quant. Spectrosc. Radiat. Transf. **130**, 4 (2013)

26. X. Liu, J.B. Jeffries, R.K. Hanson, K.M. Hinckley, M.A. Woodmansee, Development of a tunable diode laser sensor for measurements of gas turbine exhaust temperature. Appl. Phys. B **82**, 469 (2006)

27. X. Zhou, X. Liu, J.B. Jeffries, R.K. Hanson, Development of a sensor for temperature and water concentration in combustion gases using a single tunable diode laser. Meas. Sci. Technol. **14**, 1459 (2003)

28. X. Zhou, J.B. Jeffries, R.K. Hanson, Development of a fast temperature sensor for combustion gases using a single tunable diode laser. Appl. Phys. B **81**, 469 (2005)